IEEE Access
Multidisciplinary | Rapid Review | Open Access Journal

Received April 24, 2018, accepted May 28, 2018, date of publication June 4, 2018, date of current version June 29, 2018.

Digital Object Identifier 10.1109/ACCESS.2018.2843378

Mixed Reality Guided Radiofrequency Needle Placement: A Pilot Study

WEIXIN SI, XIANGYUN LIAO, YINLING QIAN, AND QIONG WANG

Shenzhen Key Laboratory of Virtual Reality and Human Interaction Technology, Shenzhen Institutes of Advanced Technology, Chinese Academy of Sciences, Shenzhen 518055, China

Corresponding author: Yinling Qian (qianyinling@gmail.com)

This work was supported in part by the Shenzhen Science and Technology Program under Grants JSGG20170414112714341 and JCYJ20160429190300857, in part by the National Natural Science Foundation of China under Grants U1613219 and 81601576, in part by the Guangdong Province Science and Technology Plan Project under Grant 2016A020220013, in part by the Science and Technology Plan Project of Guangzhou under Grant 201704020141, and in part by the China Postdoctoral Science Foundation under Grant 2017M622831.

ABSTRACT This paper presents a novel mixed reality (MR) guidance method for liver tumors radiofrequency ablation (RFA). Compared with traditional computed tomography (CT)-guided method, our system can provide a more natural and intuitive surgical mode for surgeons. In essence, our system is a holographic navigation platform, which projects a MR overlay onto the patient via HoloLens during RFA. We first reconstruct the patient-specific anatomy structure from the CT images of abdominal phantom. Then, a tailored precise registration method is employed to map the virtual-real spatial information. In addition, considering that tumor shifting during biopsy severely impacts the accuracy of RFA, our guidance system involves a motion compensation computation through data-driven physically-based modeling in holographic environment. In experiments, we conduct a user study on the comparison trial between MR-guided and CT-guided biopsy. User feedback demonstrates that our MR guidance method for needle placement procedure has the potential to simplify the operation, reduce the operation difficulty, shorten the operation time, and raise the operation precision.

INDEX TERMS Mixed reality, holographic navigation platform, motion compensation, needle placement.

I. INTRODUCTION

Radiofrequency ablation (RFA) (as shown in Fig. 1) is an widely performed technique in the treatment of liver tumor [1], and image-guided RFA nowadays is the main modality for minimally invasive therapy of primary and metastatic liver tumors. Surgeons need to master hand-eye coordination of guided imaging and needle manipulation to target an organ mass for RFA. During this procedure, a needle is first inserted through a small skin incision and then progressively advanced through tissues which is visualized by guided images. After the needle reaches the target tumor, it may transmit a periodic pulsation to the operator as the tumor has a larger stiffness and produces higher resistance to the needle.

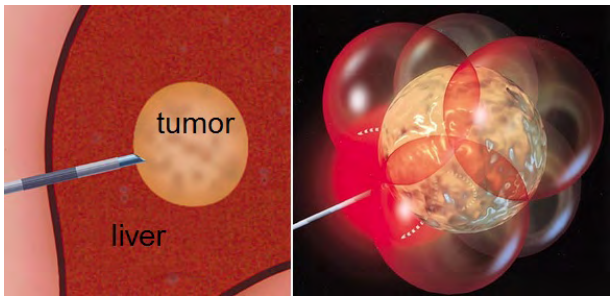

FIGURE 1. RFA of liver tumor.

Surgeons in traditional RFA are guided by the computed tomography (CT), ultrasound or magnetic resonance (MR) imaging to approach the target tumor. For a precise RFA operation, surgeons need to guarantee complete coagulation of the tumor tissue and meanwhile avoiding the injury of critical structures inside the liver. Therefore, the image modality for guidance should enable accurate planning and precise targeting of the RF applicator into the tumor [2]. However, current modalities are based on 2D images which lacks 3D structural and spatial information of the surrounding tissues. Besides, the ''Heads up'' display makes it difficult for users to smoothly coordinate their hand operations with the vision. This further increases the operation difficulty and reduces the operation precision [3]–[5]. Mixed Reality (MR) is a promising technology for surgical guidance. It can enhance

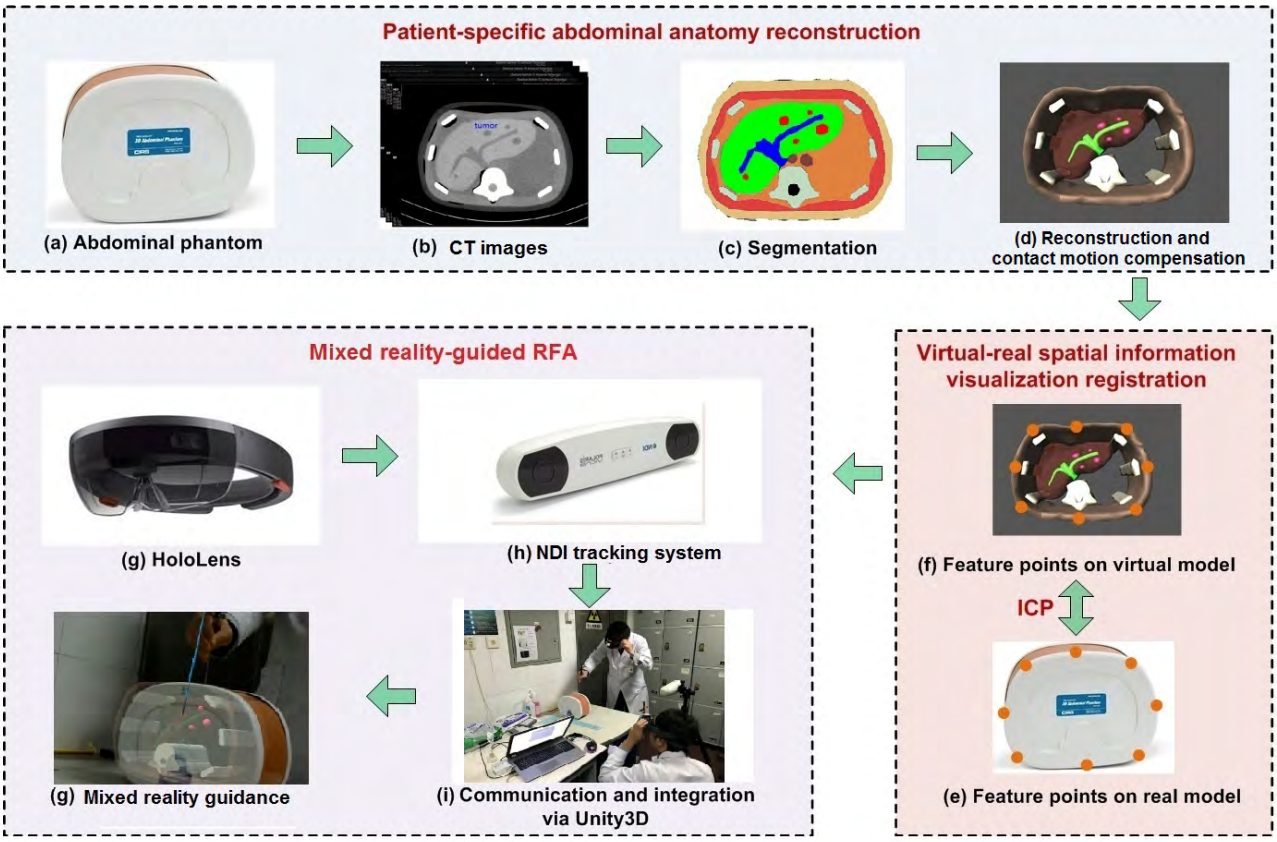

FIGURE 2. Overview of mixed reality guidance for RFA of liver tumors. We first segment the pre-operative CT images of abdominal phantom and reconstruct the 3D anatomy of liver and key surrounding structures. Meanwhile, contact motion compensation is modeled for realistic deformation and displacement estimation during the needle insertion. Then, to provide high immersive mixed reality guidance, we perform the virtual-real spatial information registration by selecting several 3D non-coplanar feature points on both real and virtual abdominal phantom, calibrating the coordinate system of Microsoft HoloLens and NDI tracking system and dynamically registering the operating needle in surgical scene. Finally, we sync two Microsoft HoloLens up for mixed reality guidance during RFA of liver tumors, which allows doctors performing the surgery collaboratively with more comprehensive information.

the surgeon's sensory experience through the fusion of imaging modalities with real object and would aid the user's perception of depth and spatial relationships in the practice environment [6], [7]. In this regard, by integrating MR into the RFA of liver tumor, surgeons can directly observe the target region while still remain cognizant of and engage in true surgical environment, which would greatly enhance the efficiency and precision of surgeons' operation.

Different from augmented reality-based systems which can only overlay the visual image on real object, mixed reality systems can provide a highly immersive holographic environment, in which the user can interact with virtual objects while the objects response to the complex interaction including the physically-based contact modeling, deformation, etc. In RFA surgery, during the needle insertion, the tumor could deform and move away as the interaction force induced by tissue-needle interaction, thus the mixed-reality based guidance that including the realistic mechanical response is essential for clinic RFA surgery. In this paper, we developed a holographic navigation platform for RFA via HoloLens, which provides a hands-free display and an overlay indicating exactly where the surgeon should operate. Our ultimate goal is to integrate the MR guidance into real RFA procedure and to assist surgeons in accurately approaching the target tumors, making the operation simpler, more efficient and more accurate. The overview of our system is as shown in Fig. 2.

The remaining of this paper is organized as follows. Section 2 reviews related work on surgical guidance for RFA and soft tissue modeling. Section 3 describes the methodology. Section 4 gives the experimental results and user study. Section 5 draws conclusion and future work.

II. RELATED WORK

A. SURGICAL GUIDANCE FOR RFA

Image-guided ablation techniques have significantly developed over the past two decades and are increasingly used to treat small tumors of liver and kidney. Many research has explored image-guided ablation of tumors and demonstrated the accuracy of image guidance. It is recommended by most guidelines as the best therapeutic choice for patients with early stage hepatocellular carcinoma [8]. An essential premise to achieve good results with percutaneous ablation therapies is the availability of precise and reliable

imaging techniques which can facilitate accurate pre-procedural planning, intraprocedural targeting, and postprocedural therapeutic assessment [9], [10]. Ultrasound (US) is actually the most widely used imaging technique for guiding percutaneous ablations, because it allows for real-time visualization of needle insertion and monitoring of the procedure and does not require ionizing radiation [11]. Moreover, a non-negligible number of liver tumors can be clearly visualized on computed tomography (CT), magnetic resonance imaging (MRI), or positron emission tomography (PET), but are completely undetectable with US because of their locations, small sizes, or echogenicity [12]–[14]. Besides, by referencing to pre-operative CT imaging, Amalou and Wood [15] adopted another modality of electromagnetic tracking, which utilizes miniature sensors integrated with RFA equipment, to guide tools in real-time. This technology was demonstrated successfully during a lung tumor ablation with accuracy of 3.9 *mm*. It is more accurate in targeting the tumor, comparing to traditional freehand needle insertion.

B. PHYSICALLY-BASED MODELING OF SOFT TISSUE

Soft tissue modeling in surgical simulation has been greatly studied in the last two decades [16], [17]. Reference [18] comprehensively overviewed physically-based deformable models used in computer graphics. The most widely used method is FEM. It can accurately describe the elastic behavior of soft tissue, which is viewed as a continuous medium composed by connected volumes. However, the mathematical formulation of FEM to describe the biomechanical material is too sophisticated for efficient computation [19]. One of the most important simplifications about FEM is the supposition that deformations and displacements are small, which leads to the theory of linear elasticity. Based on this assumption, [16], [20], [21] can be applied for efficient surgical simulation computation, but they are accurate only for small deformations and would produce visible artifacts under large deformations. To overcome this limitation, some researchers [22]–[24] proposed nonlinear models using the Total Lagrangian Explicit Dynamic algorithm (TLED), where all variables are referred to the original configuration of the system. These approaches eliminate the necessity of rotating incremental stresses before addition. Although the simulation of nonlinear bodies using these approaches is faster, the computation remains complex, and the capability for realtime deformation simulation has been only demonstrated using relatively small model [25]. Besides, [26], [27] propose composite finite element method (CFEM) to approximate a high-resolution finite element discretization of a partial differential equation by means of a smaller set of coarser elements. References [28] and [29] used composite finite element method to resolve complicated simulation domains with only a few degrees of freedom, and also to improve the convergence of geometric multigrid methods by an effective representation of complicated object boundaries at each coarser scale. In computer graphics, Nesme *et al.* [30] employed CFEM as a special kind of homogenization for resolving complicated topologies and material properties in deformable body simulation.

Alternatives to FEM that require less computational power have been investigated for surgical training and planning. Position-based dynamics [31] is widely adopted in computer graphics to achieve efficient and robust modeling and simulation of many phenomena related to deformable objects, rigid body and fluids. Müller *et al.* first proposed the position-based dynamics [31], which computes position of deformable body directly by iteratively resolving geometric constraints and provides stable control for even simple and fast explicit time integration scheme with simplicity, robustness and high efficiency [32]. Wang [33] studied the use of Chebyshev semi-iterative approach in projective and position-based dynamics, and achieve efficient dynamic simulation of deformable body. Macklin and Müller [34] presented position-based fluids, which integrated the iterative density solver into the position-based dynamics framework by formulate and solve a set of positional constraints that enforce constant density. The position-based fluids allows similar incompressibility and convergence to smoothed particle hydrodynamic (SPH), as well as large time steps and real-time computation of incompressible fluids. Deul *et al.* [35] proposed a position-based approach to achieve large-scale simulations of rigid bodies at interactive frame rates. They solved positional constraints between rigid bodies and can integrated it into other position-based methods for deformable bodies, and achieved two-way coupling with deformable bodies. Benefiting from its robustness and capability for real-time simulation, position-based dynamics can be well integrated into intraoperative guidance applications.

III. METHODOLOGY

Our system consists of several components: patient-specific abdominal anatomy reconstruction, virtual-real spatial information visualization registration and contact motion compensation.

A. PATIENT-SPECIFIC ABDOMINAL ANATOMY RECONSTRUCTION

We employ the triple modality 3D abdominal phantom (Model 057A, Computerized Imaging Reference Systems, Inc.) as the experimental object. This abdominal phantom includes artificial liver, vessels and tumors, etc., which is suitable for performing RFA for liver tumor. The accuracy of liver RF ablation simulation is greatly influenced by the anatomic structure of the abdominal phantom. Thus, the first step to develop mixed reality guidance for liver tumor RFA is to accurately reconstruct 3D geometric model of the patient-specific abdominal phantom, including the liver, vessel and tumors, which is the working area of the liver RFA procedure. The abdominal phantom was scanned by the magnetic resonance equipment. Here we adopt the Materialize Mimics software to manually segment the CT images of abdominal phantom and accurately extract different type of tissue. Afterwards, we obtain the heterogeneous structure

FIGURE 3. Phantom and needle registration. (a) and (b) represent the scenario before and after phantom calibration. (c) and (d) represent the scenario before and after needle registration.

of abdominal phantom, including skin, bone, liver, vessel and tumors.

B. VIRTUAL-REAL SPATIAL INFORMATION VISUALIZATION REGISTRATION

To obtain high immersive mixed reality guidance, we utilize the Microsoft HoloLens to overlay holographic 3D geometrical information of the hidden target objects in the real abdominal phantom, thus to enable the user to approach the target tumor in a ''see through'' style and to provide more intuitive interaction way as the real liver RFA does. To accurately realize the automatic mixed reality registration, we select several 3D non-coplanar feature points on the surface of the real abdominal phantom, and mark them on the corresponding positions of 3D reconstructed surface of abdominal phantom. First, we calibrate the coordinate system of NDI tracking system and the HoloLens platform by placing the known virtual spheres overlay with the real markers. Here the coordinates of known virtual spheres are $\mathbf{P}$ in HoloLens platform, the coordinates of real markers are $\mathbf{Q}$ in the NDI tracking system. The transformation matrix from NDI tracking coordinate system to HoloLens platform coordinate system is $\mathbf{T}$, $\mathbf{P} = \mathbf{TQ}$. After calibrating the coordinate system of NDI tracking system and HoloLens platform, we can obtain the coordinates of feature points in HoloLens platform via NDI tracking system easily. By tracking the coordinates of the selected 3D feature points on the real abdominal phantom with NDI tracking system, we employ iterative closest point (ICP)-based automatic rigid registration method to match the feature points on both virtual and real abdominal phantom, and then overlay the holographic abdominal anatomy onto the real one, thus achieving accurate automatic registration and mixed reality guidance. In addition, our system can also visualize the needle position during needle placement, which allows surgeons seeing the exact position of the needle tip. Here we create a virtual needle and perform registration with the real needle, thus enabling surgeon see the depth of the needle insertion. Specifically, we rotate the needle around a point A which can be treated as the a sphere center, then we acquire the position and direction of the marker on the needle, as well as the accurate position of point A, thus enabling us accurately perform registration between the real needle with the virtual needle. The registration of the abdominal phantom and needle is shown in Fig. 3.

C. CONTACT MOTION COMPENSATION

Tumor biopsy requires precise targeting of hepatic structures, however, this procedure is subject to soft tissue deformation and contact motion (tumor movement induced by needle insertion). To compensate the contact motion of the liver and tumor induced by the inserted needle, we need to compute the accurate soft tissue deformation and provide the updated position of the tumor with high efficiency, especially in the computation platform of Microsoft HoloLens.

Here we introduce a unified particle-based heterogeneous deformable model which is based on position-based dynamics [31] to continuously estimate the position of a moving target and guide the needle placement in real-time. Position-based dynamics was proposed to simulate realistic soft body deformation in a efficient and robust way by setting the diversified constraint for the particles to achieve corresponding desired deformation effects. Considering the limited computation resources of the Microsoft HoloLens, based on the position-based dynamics, we propose a step-by-step unified particle-based heterogeneous deformable model to compute the contact motion compensation. Our method consists of the following components:

1) HETEROGENEOUS ANATOMY CONSTRUCTION

The liver is a heterogeneous organ which consists of liver tissue, vessel and tumor. To accurately and efficiently model the deformation and movement of the heterogeneous liver, we first construct the heterogeneous anatomy of liver, as shown in Fig. 4. The surface model of abdominal phantom and liver is reconstructed directly from the segmented CT images for mixed reality guidance with rendered image of the internal structure of abdominal phantom. To construct the particle-based mechanical model of heterogeneous model, we first establish an initial hexahedral mesh that contains all the segmented CT images of abdominal phantom. Then, we define the vertices of the hexahedral mesh as the particle to represent each kind of deformable body (soft tissue, vessel and tumor). We identify each kinds of particles by its position in the segmented CT images. Taking liver soft tissue particles as an example, the particle resides in the liver soft tissue, it is defined as the liver soft tissue particles. The status of all particles are resolved with the position-based dynamics, and we adopt the MLS method [36] to represent the reconstructed surface of heterogeneous liver with their

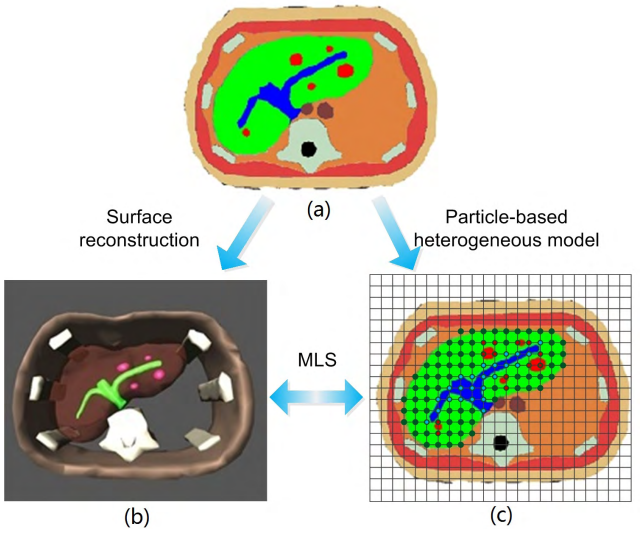

FIGURE 4. Heterogeneous anatomy construction. (a) is the manually segmented abdominal phantom CT image, (b) is the reconstructed surface of abdominal phantom, (c) is the particle-based heterogeneous anatomy of liver. Green particles represent liver soft tissue, blue particles represent vessel and red particles represent tumor.

neighboring particles, thus the deformation can be reflected on the reconstructed liver for mixed reality guidance.

2) UNIFIED PARTICLE-BASED HETEROGENEOUS DEFORMABLE MODEL

To accurately model the mechanical behavior of the heterogeneous liver with high efficiency, we propose the unified particle-based heterogeneous deformable model, which represents the liver soft tissue, vessel and tumor with unified particles, as shown in Fig. 4(c). Each kinds of particles are assigned with different attribute for position correction in the position-based dynamics. For a single kind of particles (such as liver soft tissue), C is a constraint for n particles $P = \{p_1, p_2, p_3, \ldots, p_n\}$, which satisfies $C(P) = 0$. When the external force $\mho$ exerts on the particles, the constraint C will not satisfy $C(P) = 0$ due to the updated position of all particles. To make all the particles satisfying the constraint again, we need to give a correction ΔP to the position of the particles, which satisfies $C(P + \Delta P) = 0$, and we have

$$C(P + \Delta P) \approx C(P) + \nabla_p C(P) \cdot \Delta P = 0 \tag{1}$$

where $\nabla_p C(P)$ is the constraint's partial derivatives of particles position. According to the gradient descent method, we can let the particles move along the gradient descent direction, thus we have

$$\Delta P = \lambda \nabla_p C(P) \tag{2}$$

The position correction ΔP can be derived as

$$\Delta P = -\frac{C(P)}{|\nabla_p C(P)|^2} \nabla_p C(P) \tag{3}$$

For each particle p_i,

$$\Delta_{p_i} = -s\omega_i \nabla_{p_i} C(P) \tag{4}$$

where $\omega_i = 1/m$, and

$$s = \frac{C(P)}{\sum_j \omega_j |\nabla_{p_i} C(P)|^2} \tag{5}$$

The above equations are for homogeneous deformable body simulation, while for heterogeneous liver that contains different kinds of soft tissue (liver soft tissue, vessel and tumor), we need to consider the heterogeneity of the all kinds of tissues, here we introduce a parameter k to represent the stiffness property of tissue.

$$\Delta_{p_i} = -s\omega_i \nabla_{p_i} C(P)(1 - (1 - k)^{\frac{1}{n_s}}) \tag{6}$$

where n_s is the iterative number, k is the stiffness parameter. When k is close to 0, $(1 - (1 - k)^{\frac{1}{n_s}})$ is also close to 0, thus the displacement of p_i is small, which can represent the tissue with less stiffness. For liver soft tissue, vessel and tumor, there exists three stiffness parameters k_s, k_v and k_t, respectively.

On the boundary, the liver soft tissue, vessel and tumor are connected and coupled all the time, thus we adopt the distance constraint for all particles of the heterogeneous liver, including liver soft tissue, vessel and tumor. For arbitrary two particles p_1 and p_2, the distance constraint is

$$C(p_1, p_2) = |p_1 - p_2| - d \tag{7}$$

where d is the initial distance between p_1 and p_2, $\nabla_{p_1} C(p_1, p_2) = \mathbf{n}$, $\nabla_{p_2} C(p_1, p_2) = -\mathbf{n}$, $\mathbf{n} = \frac{p_1 - p_2}{|p_1 - p_2|}$. The position corrections for p_1 and p_2 are

$$\Delta_{p_1} = -\frac{\omega_1}{\omega_1 + \omega_2} (|p_1 - p_2| - d)\, \mathbf{n}(1 - (1 - k)^{\frac{1}{n_s}}) \tag{8}$$

$$\Delta_{p_2} = +\frac{\omega_2}{\omega_1 + \omega_2} (|p_1 - p_2| - d)\, \mathbf{n}(1 - (1 - k)^{\frac{1}{n_s}}) \tag{9}$$

3) DATA DRIVEN PARAMETERS ESTIMATION

To precisely model liver deformation, we have to obtain the stiffness parameters k_s, k_v and k_t for the liver soft tissue, vessel and tumor in the unified particle-based heterogeneous liver model. It is unrealistic to find universal coefficients k_s, k_v and k_t which fit all the patients and circumstances [37]. There is an important variation of our stiffness parameter. The parameters should be selected according to individual character. It is essential to estimate the personalized parameters for clinic applications. For the abdominal phantom, during the pre-operative stage, we conduct a parameter estimation experiment with magnetic resonance imaging (MRI). We marked 25 landmarks at 4 cross sections in the abdominal phantom, and acquire 3 datasets of compression for parameters estimation through calculating the landmarks' displacement errors, as shown in Fig. 5. For each dataset for parameter estimation, deformation is calculated by Eq. 1. For the landmarks in a liver soft tissue as an example, we calculate the position correction according to Eq. 6. Supposing the measurement position correction is $\Delta^0_{p_i}$, the liver soft tissue stiffness parameter is obtained by the following equation,

$$\arg\min_{k_s, k_v, k_t} \{\| \Delta_{p_i} - \Delta^0_{p_i} \|_2\} \tag{10}$$

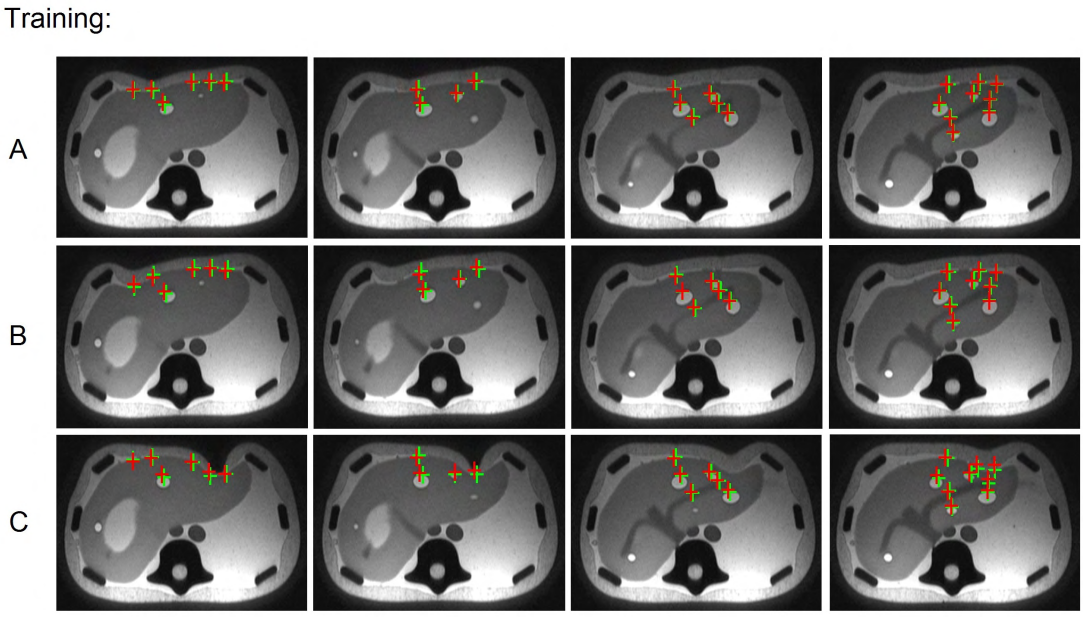

FIGURE 5. Pre-operative parameter estimation with compression experiment by magnetic resonance imaging. Green crosses are groundtruth, red crosses are calculated position with best estimated parameter.

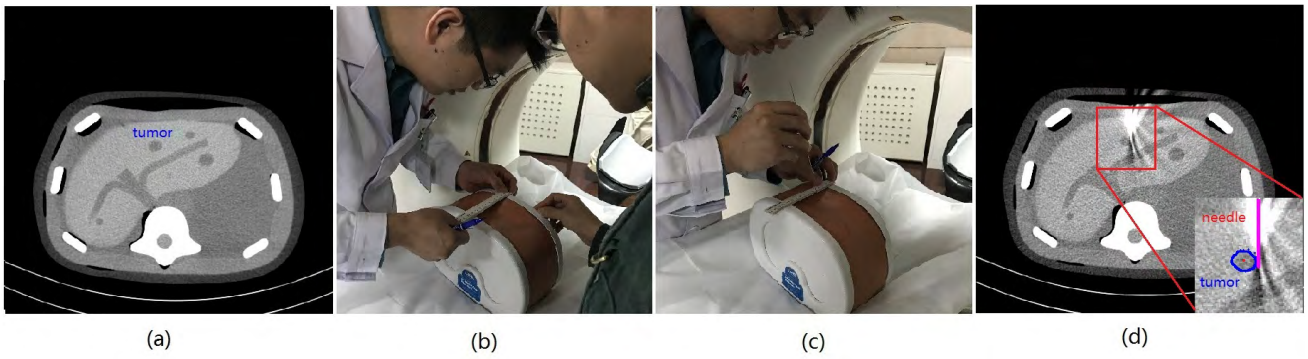

FIGURE 6. Traditional freehand needle insertion guided by the pre-opeartive CT imaging. (a) pre-opeartive CT imaging, (b)∼(c) freehand needle insertion, (d) post-operative CT imaging.

The estimation of the vessel and tumor stiffness parameters are resolved in the same way.

IV. RESULTS

We conducts a comparison trial between MR-guided needle insertion and traditional pre-operative CT imaging-guided freehand needle insertion for liver RFA as well as a user study to evaluate the face and content validity. The center of the tumor is set as the accurate target position of needle insertion. All experiments are conducted on a Microsoft HoloLens and a notebook equipped with Intel(R) i7-4702MQ CPU, 8G RAM and NVIDIA GeForce GTX750M.

A. COMPARISON TRIAL

Based on real needle insertion for liver RFA procedure, we perform needle insertion operation with the mixed reality guidance and pre-operative CT imaging guidance to test traditional freehand mode and ours for liver RFA surgery. Fig. 6 demonstrates the traditional freehand needle insertion guided by the pre-opeartive CT imaging. As shown in Fig. 6, the surgeon observes and measures the position of the liver tumor in the pre-operative CT image (Fig. 6(a)) and the phantom, and then performs freehand needle insertion on the phantom (Fig. 6(a)∼ (b)). We can observe that in Fig. 6(d), the needle failed to insert the liver tumor and pass through the liver tissue that besides the liver tumor. The error of traditional freehand needle insertion is 8.52 *mm*. The CT image guidance can only provide 2D images for the internal structure of liver, vessel and tumors. It can't provide surgeons with clear guidance and increases the difficulty for the surgeons to target the tumors, obviously inducing great risk during the RFA surgery. Besides, statistics demonstrate that the surgeons takes 15 minutes to finish the pre-operative CT scanning, tumor measurement, and takes 10 minutes to complete needle insertion.

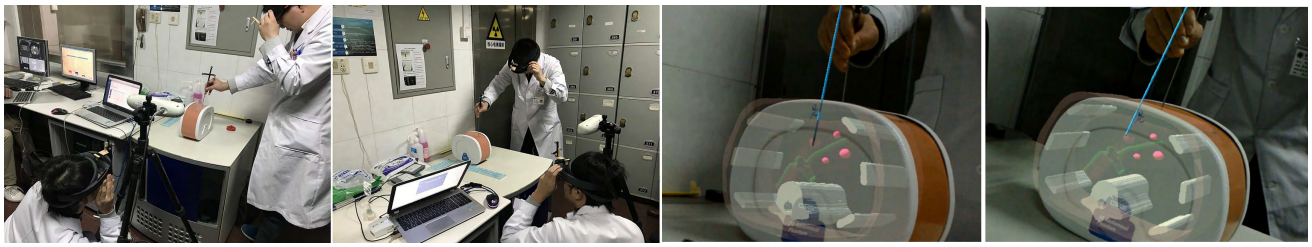

FIGURE 7. Our mixed reality-guided needle insertion for liver RFA.

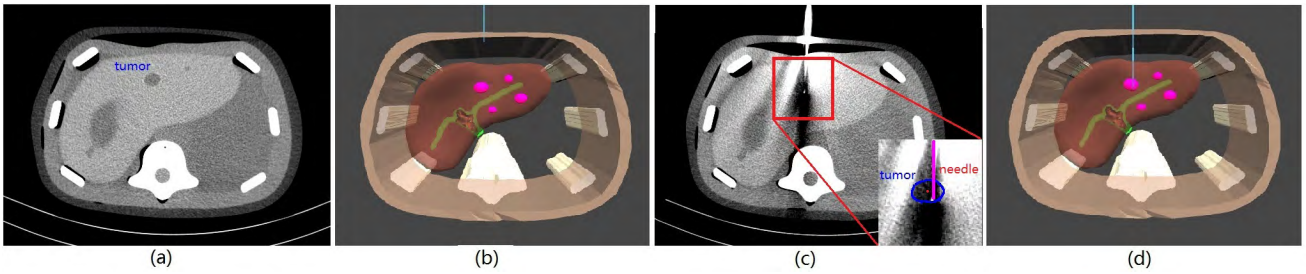

FIGURE 8. The CT imaging and reconstructed 3D models during pre-operative ((a) and (b)) and post-operative needle insertion ((c) and (d)).

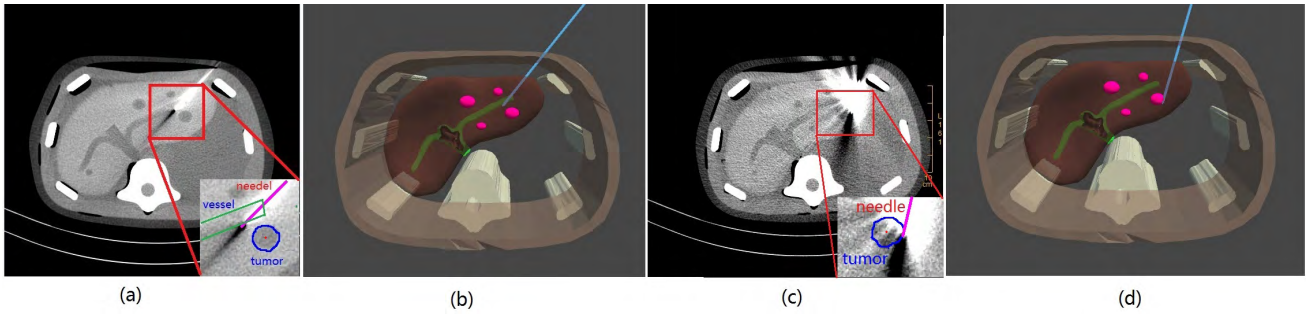

FIGURE 9. The post-operative CT imaging and reconstructed 3D models of traditional freehand needle insertion ((a) and (b)) and our mixed reality-based needle insertion. Our method can avoid damaging the vessel((c) and (d)).

Fig. 7 demonstrates the mixed reality-guided needle insertion for liver RFA. By reconstructing the abdominal phantom and registering it to the real one, we can clearly observe the internal structure of the abdominal phantom, including the target tumors, which greatly facilitates needle insertion operation by reducing the operation difficulty. Also, surgeons can insert the needle via ''See through'' display, which benefits the surgeon to coordinate their vision and operation, and thus raising the needle insertion precision. Fig. 8 illustrates the comparison of CT imaging before and after needle insertion. The error of our mixed reality-guided needle insertion is 3.23 *mm*.

Fig. 9 illustrates the post-operative CT imaging and reconstructed 3D models of traditional freehand needle insertion ((a) and (b)) and our mixed reality-based needle insertion. We can observe that traditional guidance has induced the vessel damage and the error of tradition freehand needle insertion is 13.19 *mm*, while our mixed reality guidance can avoid the needle inserting into the vessel((c) and (d)). With our mixed reality guidance, the surgeon can precisely insert the needle into the liver tumor, and the error of mixed reality-guided needle insertion is 6.98 *mm*. Besides, our method can achieve fast registration, and the surgeon takes only 5 minutes to finish the needle insertion.

In addition, we compared the needle insertion precision without tumor motion compensation with our heterogenous deformable model based motion compensation, as shown in Fig. 10. It can be observed in Fig. 10(a), without tumor motion compensation, the needle inserted into the abdominal phantom with less depth due to the absence of the tumor movement and deformation, the needle insertion accuracy is 8.41 *mm*. While with our heterogenous deformable model based motion compensation, as shown in Fig. 10(b), we take into account the tumor movement due to the needle insertion, which results in the needle insertion accuracy of 3.23 *mm*. This result demonstrates the effectiveness of our heterogenous deformable model in estimation of the tumor motion compensation.

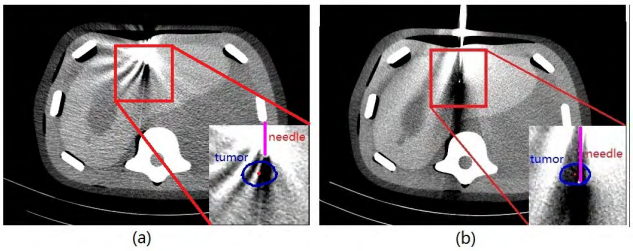

FIGURE 10. Comparison of needle insertion accuracy without (a) and with (b) heterogeneous model-based deformation compensation.

B. USER STUDY

To evaluate the performance of our mixed reality guidance and CT guidance for needle insertion in liver RFA surgery, we conduct a user study to assess the validity.

1) METHOD

The experiment was an operation comparison between the traditional CT-guided needle insertion and the mixed-reality guided needle insertion. We mainly compare the performance in aspects including the modality and clarity of the visual guidance, the difficulty and flexibility, and efficiency and the accuracy of the needle insertion.

The experiment was carried out by professional liver RFA surgeons, and each of them was required to perform the needle placement using mixed reality guidance and the traditional CT guidance, respectively. In the mixed reality guidance, the surgeons were required to be familiar with the procedures of the mixed reality guidance by practice several times wearing the Microsoft HoloLens and then perform the needle placement directly. In the traditional CT guidance, the surgeons first observed the CT images and find the target tumor, and then inserted the needle with their measurements and experiences. We calculate the whole operation time and investigate several questions to evaluate the validity of the developed system.

2) PARTICIPANTS

We recruited 10 professional surgeons who are familiar with the real CT-guided needle insertion. During the experiment, the surgeons first read the CT images before the needle insertion. We prepared an technical instruction sheet outlining goal and the operation steps of the needle insertion simulators with mixed reality guidance.

3) APPARATUS AND MATERIALS

We employ the triple modality 3D abdominal phantom as the experimental object, which includes artificial liver, vessels and tumors. The mixed reality guidance environment was constructed by the Microsoft HoloLens, the NDI tracking system and the developed method. We first segment and reconstruct the CT images of the abdominal phantom in the pre-operative stage. Then, the surgeons were shown the internal structures of the abdominal phantom, and perform the needle placement with the mixed reality guidance in the intra-operative stage. For the traditional CT-guided needle insertion, the surgeons adopt the CT equipment to scan the abdominal phantom before needle insertion. They read the CT images and measure the position of the tumor to guide the needle insertion. For the mixed reality guidance, the surgeons use the developed guidance system integrating HoloLens and NDI tracking devices to directly guided the internal position of the tumor inside the abdominal phantom.

4) PROCEDURE

In the traditional CT guidance, after observing the CT images of the abdominal phantom, the surgeons first mark on the skin of the abdominal phantom, and labeling the needle insertion position, angle and depth. Then, the surgeons carefully insert the needle along the marked position, angle and depth through the skin of the abdominal phantom. During this process, the surgeons needs to observe the 2D CT images to adjust the needle's pathway to the tumor with their personal experience.

While for the mixed reality guidance, the surgeons wear the HoloLens and directly see the mixed reality guidance image which including the internal anatomy structure of the heterogeneous liver with the help of NDI tracking system. Then, the surgeons can observe the position of the tumor and find the proper position on the skin to insert the needle. During the insertion process, the surgeons can observe the internal tumor through different viewing and thus adjusting the needle's pathway to the tumor meanwhile avoiding the liver vessel.

5) EVALUATION

After finishing the task, the surgeons were required to answer several questions we design according to the essential issues that impact the mixed reality-based surgical guidance, to evaluate the validity of our mixed reality guidance for needle insertion, meanwhile evaluating the difference between our mixed reality guidance with the CT imaging guidance. The questionnaire about our mixed reality guidance compared with the CT imaging guidance is based on 6 factors including visualization, guidance, operation efficiency, operation complexity, operation precision and overall performance. For each question, the score ranges from 0 to 10, and the higher score represents better performance. We evaluate the mixed reality guidance and the traditional CT guidance via the following questions:

- Q1: The intra-operative guided information can be efficiently obtained from the pre-operative CT images.
- Q2: The intra-operative guidance can help determine the needle insertion position, angle and depth intuitively.
- Q3: The intra-operative guidance can help avoid destroying important functional structures, such as vessels.
- Q4: The intra-operative guidance can help insert needle into the target region precisely.
- Q5: The intra-operative guidance can help insert the needle into the target tumor efficiently.
- Q6: The intra-operative guidance can help achieve the needle insertion conveniently.

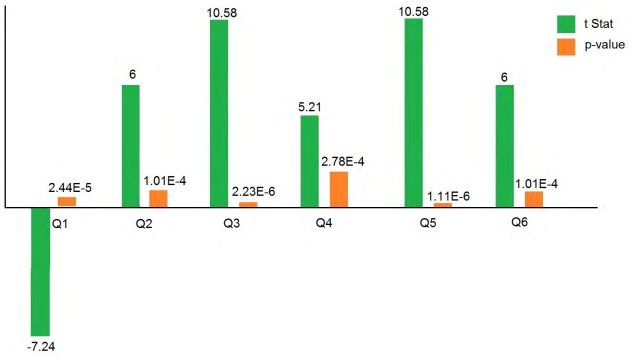

FIGURE 11. User study of comparison trial.

6) RESULTS

The results for these questions are presented in Fig. 11. We employ the p-value evaluation method with the double sample heteroscedasticity hypothesis to analysis the scores statistic data from outputs of mixed reality guidance and CT guidance, so that the statistical results can demonstrate the validity of the developed system. The t Stat is positive value and p-values are less than 0.05 for Q2 $\sim$ Q6, which indicates the mixed reality modality performs better than the CT guidance. The surgeons agreed that holographic guidance can provide more comprehensive patient-specific target region data for surgical navigation, which benefits them to precisely locate the liver tumor inside the abdominal phantom with right pathway. Besides, during needle insertion, the mixed reality guidance offers the surgeons with more intuitive surgical guidance, which results in efficient and convenient operation than that with CT guidance. Also, with mixed reality guidance, surgeons can focus on inserting the needle into target region without making use of other tools, like ruler, which allows them achieve more flexible control over the needle. However, the t Stat for Q1 is negative value and the p-value is also less than 0.05, which indicates mixed reality guidance takes more time and manpower in pre-operative processing than that in traditional CT guidance modality. This is because data representations in mixed reality guidance and CT guidance are totally different, personalized 3D anatomy reconstruction and precise registration is much harder than just quantitative measurement in technical perspective. It is worth noting that the intraoperative efficiency, convenience and precision is much more important than preoperative processing. Experimental results in Fig. 11 illustrate the developed mixed reality guidance can significantly improve the overall performance of needle insertion operation.

In addition, there are also some other limitations in current mixed reality guidance system. The view of Microsoft HoloLens is relative small and this would result in inconvenience during needle insertion because the surgeons have to adjust HoloLens frequently to make their view as large as possible. Besides, there are some delays to some extent if the movement of the needle is too fast since the dynamic registration between virtual and real needle cannot efficient enough.

V. CONCLUSION AND FUTURE WORK

This paper is to explore whether mixed reality technique has the potential to optimize the surgery procedure with the pre-operative augmented information. We perform a comparison trial to show the difference between mixed reality guidance and CT imaging guidance for needle insertion in liver RFA surgery. The user study indicated the advantages of the mixed reality guided needle insertion for liver RFA surgery, which can assist the surgeons with simpler, more efficient and more precise operation.

However, our present study can only work on the abdominal phantom, on which the registration problem can only be handled with a simple boundary conditions and lack of respiratory motion compensation that would have great impact on the position of the tumor during the surgery. To apply our method in clinic application, we need to investigate the respiratory models by constructing the relationship between the inner tumor movement with the respiratory motion on the surface skin. In this regard, our immediate plan is to achieve accurate registration in real clinic scenario and to add respiratory modeling for target shifting. Meanwhile, we are also interested in extending the mixed reality application in other guided surgeries.

ACKNOWLEDGMENT

(Weixin Si and Xiangyun Liao contribute equally to this work.)

REFERENCES

[1] D. C. Flaherty and A. J. Bilchik, "Radiofrequency ablation of liver tumors," in *Blumgart's Surgery of the Liver, Biliary Tract and Pancreas*, vol. 2, 6th ed. Amsterdam, The Netherlands: Elsevier, 2017, pp. 1436–1447.

[2] S. Clasen and P. L. Pereira, "Magnetic resonance guidance for radiofrequency ablation of liver tumors," *J. Magn. Reson. Imag.*, vol. 27, no. 2, pp. 421–433, 2008.

[3] G. Mauri *et al.*, "Real-time US-CT/MRI image fusion for guidance of thermal ablation of liver tumors undetectable with US: Results in 295 cases," *Cardiovascular Intervent. Radiol.*, vol. 38, no. 1, pp. 143–151, Feb. 2015.

[4] L. Crocetti, M. C. D. Pina, D. Cioni, and R. Lencioni, "Image-guided ablation of hepatocellular carcinoma," in *Interventional Oncology: Principles and Practice of Image-Guided Cancer Therapy*. Cambridge, U.K.: Cambridge Univ. Press, 2016, p. 91.

[5] R. L. Cazzato *et al.*, "18F-FDOPA PET/CT-guided radiofrequency ablation of liver metastases from neuroendocrine tumours: Technical note on a preliminary experience," *Cardiovascular Intervent. Radiol.*, vol. 39, no. 9, pp. 1315–1321, 2016.

[6] S. Bernhardt, S. A. Nicolau, L. Soler, and C. Doignon, "The status of augmented reality in laparoscopic surgery as of 2016," *Med. Image Anal.*, vol. 37, pp. 66–90, Apr. 2017.

[7] D. Guha, N. M. Alotaibi, N. Nguyen, S. Gupta, C. McFaul, and V. X. D. Yang, "Augmented reality in neurosurgery: A review of current concepts and emerging applications," *Can. J. Neurol. Sci.*, vol. 44, no. 3, pp. 235–245, 2017.

[8] D. J. Breen and R. Lencioni, "Image-guided ablation of primary liver and renal tumours," *Nature Rev. Clin. Oncol.*, vol. 12, no. 3, pp. 175–186, 2015.

[9] L. Tiong and G. Maddern, "Systematic review and meta-analysis of survival and disease recurrence after radiofrequency ablation for hepatocellular carcinoma," *Brit. J. Surg.*, vol. 98, no. 9, pp. 1210–1224, 2011.

[10] M. Ahmed, C. L. Brace, F. T. Lee, Jr, and S. N. Goldberg, "Principles of and advances in percutaneous ablation," *Radiology*, vol. 258, no. 2, pp. 351–369, 2011.
[11] T. Livraghi, H. Mäkisalo, and P.-D. Line, "Treatment options in hepatocellular carcinoma today," *Scand. J. Surg.*, vol. 100, no. 1, pp. 22–29, 2011.
[12] H. Rhim, M. H. Lee, Y.-S. Kim, D. Choi, W. J. Lee, and H. K. Lim, "Planning sonography to assess the feasibility of percutaneous radiofrequency ablation of hepatocellular carcinomas," *Amer. J. Roentgenol.*, vol. 190, no. 5, pp. 1324–1330, 2008.
[13] M. W. Lee *et al.*, "Targeted sonography for small hepatocellular carcinoma discovered by CT or MRI: Factors affecting sonographic detection," *Amer. J. Roentgenol.*, vol. 194, no. 5, pp. W396–W400, 2010.
[14] P. N. Kim *et al.*, "Planning ultrasound for percutaneous radiofrequency ablation to treat small (≤3 cm) hepatocellular carcinomas detected on computed tomography or magnetic resonance imaging: A multicenter prospective study to assess factors affecting ultrasound visibility," *J. Vascular Intervent. Radiol.*, vol. 23, no. 5, pp. 627–634, 2012.
[15] H. Amalou and B. J. Wood, "Electromagnetic tracking navigation to guide radiofrequency ablation (RFA) of a lung tumor," *J. Bronchol. Intervent. Pulmonol.*, vol. 19, no. 4, p. 323, 2012.
[16] S. Cotin, H. Delingette, and N. Ayache, "Real-time elastic deformations of soft tissues for surgery simulation," *IEEE Trans. Vis. Comput. Graphics*, vol. 5, no. 1, pp. 62–73, Jan. 1999.
[17] U. Meier, O. López, C. Monserrat, M. C. Juan, and M. Alcaniz, "Real-time deformable models for surgery simulation: A survey," *Comput. Methods Programs Biomed.*, vol. 77, no. 3, pp. 183–197, 2005.
[18] A. Nealen, M. Müller, R. Keiser, E. Boxerman, and M. Carlson, "Physically based deformable models in computer graphics," *Comput. Graph. Forum*, vol. 25, no. 4, pp. 809–836, 2006.
[19] G. San-Vicente, I. Aguinaga, and J. T. Celigueta, "Cubical mass-spring model design based on a tensile deformation test and nonlinear material model," *IEEE Trans. Vis. Comput. Graphics*, vol. 18, no. 2, pp. 228–241, Feb. 2012.
[20] M. Bro-Nielsen, "Finite element modeling in surgery simulation," *Proc. IEEE*, vol. 86, no. 3, pp. 490–503, Mar. 1998.
[21] M. Bro-Nielsen and S. Cotin, "Real-time volumetric deformable models for surgery simulation using finite elements and condensation," *Comput. Graph. Forum*, vol. 15, no. 3, pp. 57–66, 1996.
[22] K. Miller, G. Joldes, D. Lance, and A. Wittek, "Total Lagrangian explicit dynamics finite element algorithm for computing soft tissue deformation," *Int. J. Numer. Methods Biomed. Eng.*, vol. 23, no. 2, pp. 121–134, 2007.
[23] Z. A. Taylor, M. Cheng, and S. Ourselin, "Real-time nonlinear finite element analysis for surgical simulation using graphics processing units," in *Medical Image Computing and Computer-Assisted Intervention—MICCAI*. Berlin, Germany: Springer, 2007, pp. 701–708.
[24] O. Comas, Z. A. Taylor, J. Allard, S. Ourselin, S. Cotin, and J. Passenger, "Efficient nonlinear FEM for soft tissue modelling and its GPU implementation within the open source framework SOFA," in *Biomedical Simulation*. Berlin, Germany: Springer, 2008, pp. 28–39.
[25] G. R. Joldes, A. Wittek, and K. Miller, "Suite of finite element algorithms for accurate computation of soft tissue deformation for surgical simulation," *Med. Image Anal.*, vol. 13, no. 6, pp. 912–919, 2009.
[26] W. Hackbusch and S. A. Sauter, "Composite finite elements for the approximation of PDEs on domains with complicated micro-structures," *Numer. Math.*, vol. 75, no. 4, pp. 447–472, 1997.
[27] S. A. Sauter and R. Warnke, "Composite finite elements for elliptic boundary value problems with discontinuous coefficients," *Computing*, vol. 77, no. 1, pp. 29–55, 2006.
[28] T. Preusser, M. Rumpf, and L. O. Schwen, "Finite element simulation of bone microstructures," in *Proc. 14th Finite Element Workshop*, 2007, pp. 52–66.
[29] F. Liehr, T. Preusser, M. Rumpf, S. Sauter, and L. O. Schwen, "Composite finite elements for 3D image based computing," *Comput. Vis. Sci.*, vol. 12, no. 4, pp. 171–188, 2009.
[30] M. Nesme, P. G. Kry, L. Jeřábková, and F. Faure, "Preserving topology and elasticity for embedded deformable models," *ACM Trans. Graph.*, vol. 28, no. 3, p. 52, 2009.
[31] M. Müller, B. Heidelberger, M. Hennix, and J. Ratcliff, "Position based dynamics," *J. Vis. Commun. Image Represent.*, vol. 18, no. 2, pp. 109–118, 2007.
[32] J. Bender, M. Müller, M. A. Otaduy, M. Teschner, and M. Macklin, "A survey on position-based simulation methods in computer graphics," *Comput. Graph. Forum*, vol. 33, no. 6, pp. 228–251, 2014.
[33] H. Wang, "A chebyshev semi-iterative approach for accelerating projective and position-based dynamics," *ACM Trans. Graph.*, vol. 34, no. 6, p. 246, 2015.
[34] M. Macklin and M. Müller, "Position based fluids," *ACM Trans. Graph.*, vol. 32, no. 4, p. 104, 2013.
[35] C. Deul, P. Charrier, and J. Bender, "Position-based rigid-body dynamics," *Comput. Animation Virtual Worlds*, vol. 27, no. 2, pp. 103–112, 2016.
[36] M. Pauly, R. Keiser, L. P. Kobbelt, and M. Gross, "Shape modeling with point-sampled geometry," *ACM Trans. Graph.*, vol. 22, no. 3, pp. 641–650, 2003.
[37] L. E. Bilston, "Brain tissue mechanical properties," in *Biomechanics of the Brain*, vol. 3. New York, NY, USA: Springer, 2011, pp. 69–89.

WEIXIN SI is currently an Assistant Researcher with the Shenzhen Key Laboratory of Virtual Reality and Human Interaction Technology, Shenzhen Institutes of Advanced Technology, Chinese Academy of Sciences. His research interests include virtual reality, augmented reality, mixed reality applications in medicine, and physically-based simulation.

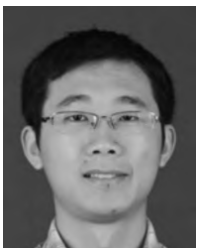

XIANGYUN LIAO is currently a Post-Doctoral Researcher with the Shenzhen Key Laboratory of Virtual Reality and Human Interaction Technology, Shenzhen Institutes of Advanced Technology, Chinese Academy of Sciences. His research interests include virtual reality, physics-based modeling, and medical imaging.

YINLING QIAN is currently a Post-Doctoral Researcher with the Shenzhen Key Laboratory of Virtual Reality and Human Interaction Technology, Shenzhen Institutes of Advanced Technology, Chinese Academy of Sciences. His research interests include virtual reality, augmented reality, and physics-based modeling.

QIONG WANG is currently an Associate Researcher with the Shenzhen Institute of Advanced Technology, Chinese Academy of Sciences. Her research interests include VR applications in medicine, visualization, medical imaging, human-computer interaction, and computer graphics.